JOURNAL OF MATERIALS SCIENCE **36** (2001) 4739–4743

Thermal decomposition study of electrodeposited Fe-C and Fe-Ni-C alloys by differential scanning calorimetry

A. S. M. A. HASEEB*, M. ARITA, Y. HAYASHI
Department of Materials Science and Engineering, Kyushu University, 6-10-1 Hakozaki, Fukuoka 812-8581, Japan
E-mail: haseeb@mme.buet.edu

Fe-0.96mass%C and Fe-15.4mass%Ni-0.70mass%C alloys with hardness of 810 and 750 HV respectively have been electrodeposited at 50°C from sulphate based baths containing a small amount of citric acid and L-ascorbic acid. Differential scanning calorimetry of the electrodeposited samples has been carried out in the temperature range of 293–725 K in argon atmosphere. Electrodeposited pure Fe is also investigated for comparison purposes. The DSC curves of both alloys contain two exothermic peaks: at about 411 K and 646 K for the Fe-C alloy, and 388 K and 639 K for the Fe-Ni-C alloy. These peaks are irreversible and do not appear during a second thermal cycling. The lower temperature peaks (designated as I) have been attributed mainly to the formation of ε/η-Fe_2C (first stage of tempering), while the higher temperature peaks (designated as III) are ascribed predominantly to θ-Fe_3C formation (third stage of tempering). The presence of these peaks in the DSC curves confirms that electrodeposited Fe-C and Fe-Ni-C alloys are in a metastable state, where carbon atoms are entrapped in the iron lattice. The decomposition sequence of electrodeposited Fe-C and Fe-Ni-C alloys is found to follow the same general pattern as that of thermally prepared martensite. Attempt has been made to estimate the activation energy values for the reactions associated with the DSC peaks of the electrodeposited alloys and these values are compared with the available data on thermally prepared martensite.

1. Introduction

Steels, the most important of all structural materials, are basically alloys of iron and carbon. The ability of Fe-C based alloys to transform into a hard martensitic structure with high hardness upon proper heat treatment is one of the main reasons for their wide spread use. In industrial practice, hard martensitic structure is achieved by heating steels to a temperature around 850°C or higher followed by rapid quenching. This process is energy consuming, environmentally unfriendly, and can cause distortion in complex machine components. Therefore, achieving hard iron-carbon based alloys through low temperature processing routes can be rather attractive from practical as well as theoretical points of view. Recently, it was reported that hard Fe-C alloys with 0.43–1.26 mass% C can be electrodeposited directly at around room temperature (50°C) from sulfate-based baths containing a small amount of citric acid and L-ascorbic acid [1]. The hardness of the electrodeposited alloy (around 800 HV) was found to be similar to that of the thermally prepared Fe-C martensite. However, X-ray diffraction study revealed [1] that the tetragonality of the electrodeposited Fe-1.21 mass%C alloy is very small, its c/a axis ratio being only 1.005; while this ratio is 1.059 for the thermally prepared martensite of similar composition. Further, in a more recent work [2], no tetragonality was observed in electrodeposited Fe-C and Fe-Ni-C alloys. In addition, traces of epsilon carbide were detected in electrodeposited Fe-C alloy (although not in Fe-Ni-C alloy). These suggest that hard electrodeposited Fe-C alloys are likely to exist in a state that is ahead of the freshly quenched state of martensite (advanced stage of tempering). To gain further insight into the nature of electrodeposited Fe-C and Fe-Ni-C alloys, their decomposition behaviour is investigated by differential scanning calorimetry (DSC) in the present work. The decomposition sequence of electrodeposited alloys is discussed and compared with the available literature data on that of their thermally prepared counterparts.

2. Experimental

Electrodeposition of the samples was carried out galvanostatically at 20 $mA \cdot cm^{-2}$ for six hours in still

* *Permanent Address*: Department of Materials and Metallurgical Engineering, Bangladesh University of Engineering and Technology (BUET), Dhaka 1000, Bangladesh.

baths maintained at $50 \pm 2^{\circ}$C. The deposition cell used was a typical three-electrode type assembly having a Ag/AgCl reference electrode. The base electrolyte contained 0.43 kmole $\cdot$ m^{-3} $FeSO_4 \cdot 7H_2O$, bath pH being adjusted to 2.5 ± 0.1 with sulfuric acid. For the Fe-C alloy deposition, 5.7×10^{-3} kmol $\cdot$ m^{-3} citric acid ($C_6H_8O_7 \cdot H_2O$) and 1.7×10^{-2} kmol $\cdot$ m^{-3} L-ascorbic acid ($C_6H_8O_6$) were added to the base electrolyte. The Fe-Ni-C alloy was deposited by adding 0.19 kmol $\cdot$ m^{-3} $NiSO_4 \cdot 6H_2O$ to the Fe-C deposition bath mentioned above. For comparison, iron was deposited from the base electrolyte. Copper sheets with an exposed area of 20 mm $\times$ 20 mm were used as substrates, while interstitial free (IF) iron sheet was used as the sacrificial counter electrode. After the deposition, the samples were peeled off from the substrate and stored in a desiccator before the DSC experiments. Deposition was carried out for about six hours, which yielded sample thicknesses of around 60–70 μm. Chemical analysis of the deposits was carried out by inductively coupled plasma (ICP) spectroscopy (Shimadzu ICPS 1000 IV) for nickel and by evolved gas analysis technique (Horiba E MIA-110) for carbon.

Differential scanning calorimetry was performed on as-deposited samples in a Rigaku Thermoplus DSC 8270 apparatus. Sample weighing 36.2 mg was placed in an alumina crucible. Alumina sample of the same weight put in another alumina crucible served as the reference. Experiments were performed in the range of 293 to 725 K using a heating rate of 0.17 K $\cdot$ s^{-1}. Heating was carried out in an inert atmosphere created by flowing argon gas (99.999% purity) through the chamber at rate of 1.67 ml $\cdot$ s^{-1}. For a couple of experiments, DSC curves were recorded after the specimens were heated to 1173 K at a rate of 0.17 K $\cdot$ s^{-1} and cooled to room temperature at 0.33 K $\cdot$ s^{-1}.

3. Results and discussion

Chemical analysis revealed that the electrodeposited Fe-C alloy contains 0.96 mass% carbon while the Fe-Ni-C alloy contains 15.4 mass% nickel and 0.70 mass% carbon. The Fe-C and Fe-Ni-C alloys possess a Vickers microhardness of 810 and 750 HV respectively. The hardness of the electrodeposited alloys is comparable to that of thermally quenched steels.

Fig. 1a, b and c respectively show the DSC curves for the electrodeposited Fe, Fe-C and Fe-Ni-C alloys. The curves for both alloys exhibit two exothermic features designated by I and III (reason for such designation will be evident later) that are absent in the curve for Fe. The first exothermic peak (I) for Fe-C alloy appears at about 411 K, while the second, much more pronounced one (peak III) appears at around 646 K (Fig. 1b). In the case of Fe-Ni-C alloy, the peaks appear approximately at 388 K and 639 K respectively (Fig. 1c). Peak I for Fe-C is relatively narrow and weak as compared to that of Fe-Ni-C. But the peak III for Fe-C is much more intense than that of Fe-Ni-C. In Fig. 2a and b are shown the DSC curves for Fe-C and Fe-Ni-C alloys respectively obtained during a second run. These samples were heated to 1173 K followed by cooling to room temperature prior to the second heating cycle. It is seen

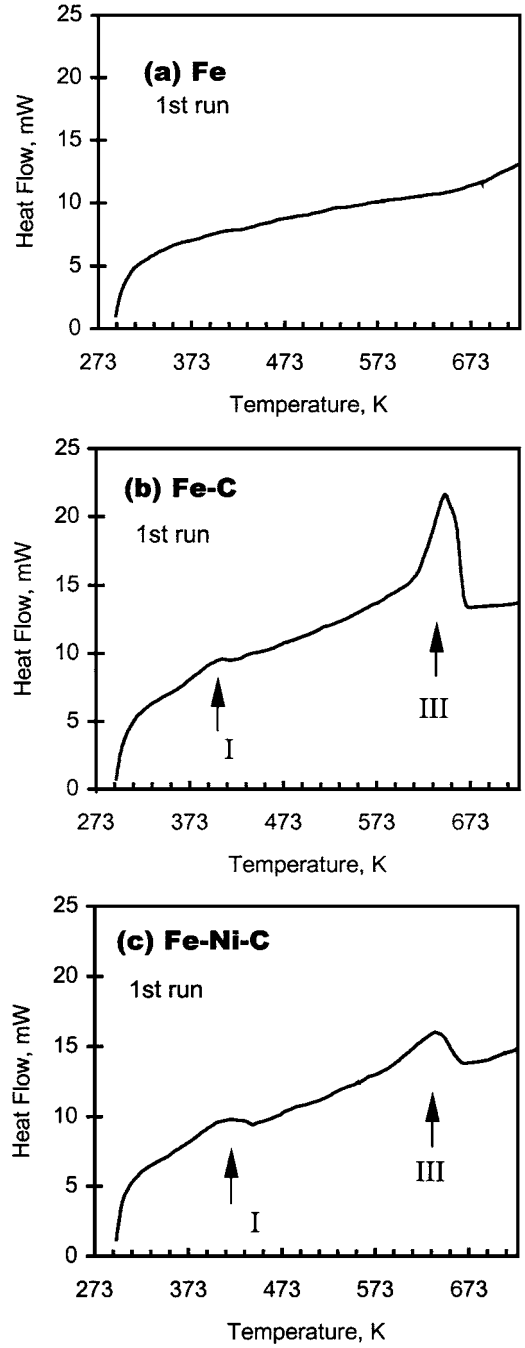

Figure 1 DSC scans of electrodeposited (a) Fe, (b) Fe-C and (c) Fe-Ni-C alloys. 1st run: scan rate, 0.17 K $\cdot$ s^{-1}. Argon atmosphere.

in Fig. 2 that none of the exothermic peaks appears in the DSC curves of the alloys during the second run. This indicates that the transformations that these exothermic peaks in the DSC curves of the electrodeposited alloys represent are irreversible and characteristics of the nature of the electrodeposited state.

Detailed structural investigations on the decomposition during heating of thermally prepared martensite have been done in the past [3, 4]. Tempering of martensite was found to proceed via several stages. At low aging temperatures, carbon atoms redistribute in the martensite matrix resulting in their segregation and clustering. This is the pre-precipitation stage. In the first stage of tempering (stage I), ε/η-Fe_2C carbide precipitates. The second stage (stage II) involves the transformation of any retained austenite. In the

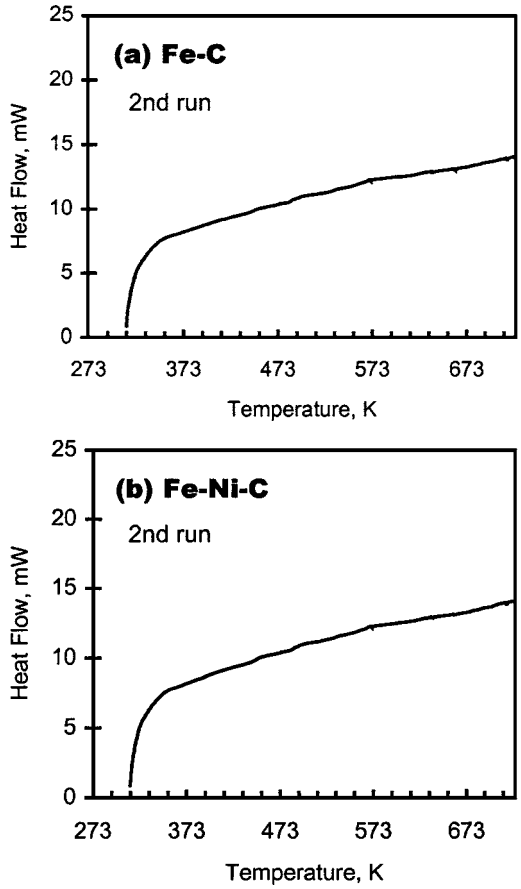

Figure 2 DSC scans of (a) Fe-C and (b) Fe-Ni-C alloys that were taken after both alloys were heated to 1173 K at 0.17 $K \cdot s^{-1}$ and cooled to room temperature at 0.33 $K \cdot s^{-1}$. 2nd run: scan rate, 0.17 $K \cdot s^{-1}$. Argon atmosphere.

third stage (stage III), precipitation of χ-Fe_5C_2 carbide and eventually the stable θ-Fe_3C takes place. Each of the above reactions involves evolution of heat. A number of workers studied the decomposition of thermally prepared martensite by thermal analysis methods, including DSC and dilatometry [5–9]. Mittemeijer *et al*. [6] discussed in detail the DSC curve for Fe-1.1 mass%C martensite obtained by quenching in brine and subsequently in liquid nitrogen. They could identify each of the above stages of tempering in the DSC curve. In the range of temperature (300–773 K) studied, they found as many as four exothermic peaks at approximate positions: 366 K, 425 K, 569 K and 590 K respectively. The weak peak at 366 K was linked to carbon distribution (segregation and clustering), while the peak at 425 K was attributed to ε/η-Fe_2C formation. Since the thermally prepared martensite contained retained austenite, the decomposition of the latter manifested itself as the peak at 569 K. The peak at 590 K was assigned to the formation of θ-Fe_3C.

Taking into account the above results on the decomposition of thermally prepared martensite, the peaks present in the DSC curves of electrodeposited Fe-C and Fe-Ni-C alloys can now be assigned. The first exothermic peak (peak I) in the electrodeposited samples is ascribed mainly to the formation of ε/η-Fe_2C, so-called first stage of tempering. Peak I in both cases is, however, rather broad and appears to be an overlap of more than just one peak particularly at the low temperature side. This peak is therefore believed to represent overlapping carbon redistribution reactions as well. The higher temperature peak (III) is attributed to the formation of θ-Fe_3C that occurs in the third stage of tempering. Peak III also appears to be composed of more than one overlapping peak. Previous study [10] on the decomposition of electrodeposited alloys identified the precipitation of χ-Fe_2C_5 along with θ-Fe_3C. Thus peak III might also include the heat evolution caused by χ-Fe_2C_5 formation. The absence of the austenite phase was confirmed in the electrodeposited Fe-C and Fe-Ni-C alloys by XRD [2] and Mössbauer spectroscopy [10] earlier. Therefore, no exothermic peak representing the transformation of austenite, that constitute the second stage of tempering of thermally prepared martensite, is expected in the DSC curve of the electrodeposited alloys.

The heat evolution associated with the peaks is given for both alloys in Table I. It is seen that in the case of ε/η-Fe_2C formation (peak I), the heat generation is relatively lower in Fe-C as compared with that in Fe-Ni-C. This is consistent with the earlier XRD result [2] which shows that the Fe-C alloy already contains traces of ε/η-Fe_2C in the as-deposited state, while Fe-Ni-C alloy does not contain any carbide. The presence of peak I in the DSC curve of Fe-C alloy at the same time indicates that, although the alloy contains traces of ε/η-carbide, the first stage of tempering is not yet complete in the as-deposited state. On the other hand, heat evolution is much higher in Fe-C alloy in the case of peak III representing the formation of θ-Fe_3C. The higher amount of heat generation in Fe-C alloy in the case of peak III is also consistent with the XRD result [2] which shows that annealing causes the formation of rather higher amount of θ-Fe_3C in Fe-C alloy compared with Fe-Ni-C. DSC results thus corroborate the previous XRD results that electrodeposited Fe-Ni-C alloy is more resistant to tempering than Fe-C alloy. The higher amount of carbon in the Fe-C alloy might as well result in greater amount of heat evolution under peak III.

The composite nature of the peaks does not allow an accurate determination of activation energy of reaction accompanying them. Nevertheless, an attempt was made to obtain a rough estimate of average activation energy associated with peaks I and III using the Coats-Redfern-Sestak method [11]. The Coats-Redfern-Sestak formalism, which allows the determination of activation energy from a single DSC curve, essentially takes the following form:

$$\ln[\{-\ln(1 - C/C_0)\}/\{T^{2n}\}] = -n\ \ln(\alpha) - nE/RT + n\ln(K_0R/nE)$$

TABLE I Heat evolution associated with the peaks

Sample	Heat evolution associated with peaks, $J \cdot g^{-1}$	
	Peak I (peak position)	Peak III (peak position)
Fe-0.96mass%C	3.41 (414 K)	79.64 (646 K)
Fe-15.4mass%Ni-0.70 mass%C	10.38 (388 K)	28.35 (639 K)

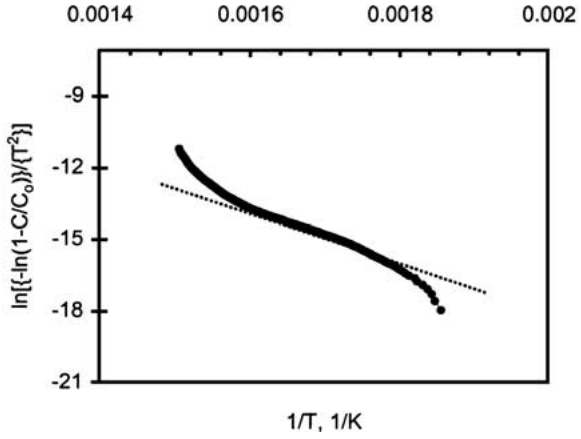

Figure 3 A typical plot of $\ln[\{-\ln(1-C/C_0)\}/\{T^2\}]$ versus $1/T$. Fe-C alloy, peak III.

where,

$C/C_0 =$ volume fraction transformed
$T =$ temperature
$n =$ order of reaction
$\alpha =$ heating rate in the DSC experiment
$E =$ activation energy
$K_0 =$ rate constant

At a constant α, the slope of the plot of $\ln[\{-\ln(1-C/C_0)\}/\{T^{2n}\}]$ versus $1/T$ can be used to calculate the activation energy, E. Fig. 3 shows an example of such a plot. The volume fraction transformed was found out by integrating the respective peak and the order of the reaction was assumed to be 1 [7]. It is seen that the middle portion of the plot fits to a straight line and was used for the present calculation of activation energy. Activation energy values thus obtained for the peaks I and III are shown in Table II. The order of magnitude of the activation energy is worth noting, without giving particular emphasis on a certain value. These values can be compared with the activation energy of some basic rate determining processes that can occur during tempering as given in Table III. One would tend to find that the present range of values is more close to the activation energy for carbon diffusion.

Activation energy values found in the literature [6, 8, 9, 12, 15–18] for the first stage of tempering of thermally prepared martensite varies within a wide range, 33–125 kJ · mol^{-1}. The activation energy for the clustering of carbon atoms during pre-precipitation stage was found to be 79 kJ · mol^{-1} [6]. The values obtained in the present case for stage I (Table II) lie within the range reported in the literature. Carbon diffusion is generally thought to be the rate determining step during the first stage of tempering [8, 12, 15–18]. However Mittemeijer *et al*. [6], who obtained activation energy value on the higher side of the above range, argued that pipe diffusion of Fe could be the rate determining step. As for the third stage of tempering, Tomita [7] and Read [8] whose calculated activation energy lies within 81.85–96.0 kJ · mol^{-1} suggested carbon diffusion as the rate controlling step. Mittemeijer *et al*. [6], on the other hand, found an activation energy of 203 kJ · mol^{-1} by dilatometry for the third stage of tempering and suggested iron volume diffusion and to a smaller extent pipe diffusion as the rate determining steps (see values in Table III). Given the fact that different theoretical formalisms, and experimental approaches and parameters were used by different investigators while determining the activation energy, a rigorous, one to one comparison of data may not be wise. However, from the range of activation energy found out in the present work and the data available in the literature, it can be safely concluded that carbon diffusion as a rate determining step plays an important role during the tempering of electrodeposited Fe-C and Fe-Ni-C alloys.

TABLE II Calculated activation energy of the reactions

	Activation energy, kJ · mol^{-1}	
Sample	Peak I	Peak III
Fe-0.96mass%C	86	91
Fe-15.4mass%Ni-0.70mass%C	83	97

TABLE III Activation energy of some basic processes that can occur during the tempering of martensite

Basic process	Activation energy, kJ · mol^{-1}	References
C diffussion in ferrite	78.0	[11]
C diffusion in martensite	81.1	[12]
Fe diffusion through dislocations (pipe diffusion)	134.0	[13]
Volume diffusion of Fe	251.0	[14]

4. Conclusions

The DSC curves of electrodeposited Fe-0.96mass%C and Fe-15.4mass%Ni-0.70mass%C in the range of 293–725 K contain two exothermic peaks: at about 411 K and 646 K for Fe-C alloy, and 388 K and 639 K for Fe-Ni-C alloy. These peaks are irreversible and do not appear during a second thermal cycling. The lower temperature peaks (designated as I) have been attributed mainly to the formation of ε/η-Fe_2C (first stage of tempering), while the higher temperature peaks (designated as III) are ascribed to θ-Fe_3C formation (third stage of tempering). The presence of these peaks in the DSC curves confirms that electrodeposited Fe-C and Fe-Ni-C alloys are in a metastable state, where carbon atoms are entrapped in the iron lattice. The decomposition sequence of electrodeposited Fe-C and Fe-Ni-C alloys if found to follow the same general pattern as that of thermally prepared martensite. DSC data corroborate the earlier XRD results that Fe-Ni-C alloy is more resistant to tempering than the Fe-C alloy. The range of activation energy estimated for reactions associated with the peaks suggests that carbon diffusion as a rate determining step plays an important role during the tempering of electrodeposited Fe-C and Fe-Ni-C alloys.

Acknowledgements

One of the authors (ASMAH) would like to thank Japan Society for the Promotion of Science for a visiting fellowship and BUET for sabbatical leave.

References

1. M. IZAKI and T. OMI, *Metall. Mater. Trans.* **27A** (1996) 483.
2. A. S. M. A. HASEEB, Y. HAYASHI and M. MASUDA, Paper # F8.6, Presented at the Materials Research Society (MRS) Spring 2000 Meeting, 24–28 April 2000, San Francisco, USA.
3. S. NAGAKURA, Y. HIROTSU, M. KUSUNOKI, T. SUZUKI and Y. NAKAMURA, *Met. Trans.* **14A** (1983) 1025.
4. A. M. SHERMAN, G. T. ELDIAS and M. COHEN, *ibid.* **14A** (1983) 995.
5. E. J. MITTEMEIJER, A. VAN GENT and P. J. VAN DER SCHAAF, *ibid.* **17A** (1986) 1441.
6. E. J. MITTEMEIJER, L. CHENG, P. J. VAN DER SCHAAF, C. M. BRAKMAN and B. M. KOREVAAR, *ibid.* **19A** (1988) 925.
7. Y. TOMITA, *Mater. Sci. Tech.* **4** (1988) 977.
8. H. G. READ, *Scripta Mater.* **37** (1997) 151.
9. M. J. VAN GENDEREN, M. ISAC, A. BÖTTGER and E. J. MITTEMEIJER, *Metall. Mater. Trans.* **28A** (1997) 545.
10. A. S. M. A. HASEEB, T. NISHIDA, M. MASUDA and Y. HAYASHI, *Scripta Mater.* **44** (2001) 519.
11. N. AFIFY, *J. Non-Crystalline Solids* **142** (1992) 247.
12. J. R. G. DA SILVA and R. B. MCLELLAN, *Mater. Sci. Eng.* **26** (1976) 83.
13. M. HILLERT, *Acta Metall.* **7** (1959) 653.
14. M. COHEN, *Trans. JIM* **11** (1970) 145.
15. F. S. BUFFINGTON, K. HIRANO and M. COHEN, *Acta Metall.* **9** (1961) 434.
16. B. L. AVERBACH and M. COHEN, *Trans. Amer. Soc. Metals* **41** (1949) 1024.
17. C. S. ROBERTS, B. L. AVERBACH and M. COHEN, *ibid.* **45** (1953) 576.
18. B. S. LEMENT and M. COHEN, *Acta Metall.* **4** (1956) 469.

Received 2 June 2000
and accepted 15 May 2001